Solvatochromic shifts of polar and non-polar molecules in ambient and supercritical water: A sequential quantum mechanics/molecular mechanics study including solute-solvent electron exchange-correlation

Haibo Ma and Yingjin Ma

Citation: J. Chem. Phys. **137**, 214504 (2012); doi: 10.1063/1.4769124
View online: http://dx.doi.org/10.1063/1.4769124
View Table of Contents: http://jcp.aip.org/resource/1/JCPSA6/v137/i21
Published by the AIP Publishing LLC.

Solvatochromic shifts of polar and non-polar molecules in ambient and supercritical water: A sequential quantum mechanics/molecular mechanics study including solute-solvent electron exchange-correlation

Haibo Ma[a] and Yingjin Ma
Institute of Theoretical and Computational Chemistry, Key Laboratory of Mesoscopic Chemistry of MOE, School of Chemistry and Chemical Engineering Nanjing University, Nanjing 210093, China

(Received 26 August 2012; accepted 13 November 2012; published online 6 December 2012)

Polar and non-polar solutes (acetone and benzene) dissolved in ambient water and supercritical water are investigated theoretically using a sequential quantum mechanics (QM)/molecular mechanics (MM) method which combines classical molecular dynamics simulations and QM/MM calculations. From the detailed analysis of the dependence of the QM region size and point charge background region size as well as the different functionals, it is found that the inclusion of the solvent molecules within the first solvation shell into the QM region to account for the exchange-correlation between a solute and neighboring solvent molecules is important for the highly accurate spectral shift calculations, especially vital for the non-polar solutes whose interactions with the solvents are dominated by the quantum dispersions. At the same time, sufficiently large surrounding partial charge region ($r_{cutoff} \geq 15$ Å) as well as the functional corrections to describe the long-range dispersion-corrections are also essential for the study of the electronic excited states in condensed phase. Our calculated solvatochromic shift values and their density dependencies at ambient and high temperature conditions are found to be in good agreements with experimental observations. This indicates that sound theoretical studies of solvatochromic shift can be achieved provided that a reasonable computational scheme with sufficiently large N_{water}^{QM} and r_{cutoff} values is implemented. We also find both of aqueous acetone and aqueous benzene under high temperatures present three distinctive regions: low-density gas-like region, supercritical region, and high-density liquid-like region. The plateau behavior of solvatochromic shift in the supercritical region can be ascribed to the solvent clustering around the solute, which is a fundamental phenomenon of supercritical fluids (SCFs). The density dependence of our calculated coordination number of the first solvation shell nicely reproduces the trend of spectral shift and verifies the solvent clustering phenomenon of SCFs and its relationship with SCF's physicochemical properties. © *2012 American Institute of Physics*. [http://dx.doi.org/10.1063/1.4769124]

I. INTRODUCTION

While solvents can have strong influences on solubility, stability, and reaction rates, solvent effect draws a substantial number of attentions as a potential thermodynamic and kinetic control over a chemical reaction. In the recent decades, the study of supercritical fluids (SCFs) has been a research focus because of its important potential as an environmentally benign green alternative to toxic organic solvents.[1–4] Nowadays, carbon dioxide and water are the two mostly studied supercritical solvents due to their abundance and important roles in biological systems as well as in many industrial applications.[5,6]

A special advantage for the application of SCFs is that their physicochemical properties can be modulated through the minor variation of the temperature of pressure. For example, the solubilities of polar or non-polar molecules in SCFs can be tuned because the solvent polarity of SCF can be changed with the varied temperature or pressure. Consequently, the study of the density dependence and the temperature dependence of the physicochemical properties of SCFs is very important for the further understanding and optimization of SCFs as novel green solvents.[7–14] Solvatochromic probes are currently widely used as indicator of solvent polarity because they can provide valuable information on the magnitude and dynamics of the intermolecular interaction between a solute and the solvents.[15] Therefore, solvatochromic shifts of various organic chromophores dissolved in solvents have also been introduced to the study of SCFs by probing the density or temperature dependence of SCFs' physicochemical properties.[16–19]

However, calculations on the electronic excited states in the condensed phase remain a huge challenge to the theoretical chemistry community.[20] The increased number of nuclear and electronic degrees relative to the gas phase and the more delocalized nature of the electronic excited states comparing to that of the ground state make the accurate fully quantum mechanical calculations of the electronic exited states on a condensed-phase system unfeasible long before the system can approach the bulk. On the basis of the traditional non-equilibrium solvation theory in continuum model, the bulk solvent effects can be described with an implicit solvation model such as the self-consistent reaction field,[21]

[a]Author to whom correspondence should be addressed. Electronic mail: haibo@nju.edu.cn.

polarizable continuum model,[22] surface and simulation of volume polarization for electrostatics,[23] or conductor-like solvation model.[24] While the advantage in reduced computation costs with an implicit solvation model is considerable, no microscopic information can be provided and solvent-specific effects such as hydrogen bonding cannot be well reproduced. For the study of solutions under sub-critical and supercritical conditions, the appropriate definitions of parameters in an implicit solvation model such as dielectric constant and cavity radius are also questionable. Another group of approaches for the study of the electronic structure of solvated molecules that is getting popular uses a combined quantum mechanics/molecular mechanics (QM/MM) hybrid approach[25] in which the most important part of the problem is treated by quantum mechanics and the surrounding environment is normally described by the empirical force fields of discrete solvent molecules. A major drawback of empirical force field methods is that their performances are highly dependent on the empirically fitted parameters and the best parameters are usually not well defined. Another concern of empirical force field methods is that many molecules of interest to a chemist are outside the range of molecules for which current force fields are parameterized. In order to overcome these drawbacks, the effective fragment potential (EFP) method[26–28] has been developed to represent the solvent part. In the EFP method, each solvent molecule is represented by an effective fragment whose parameters are all determined from a preparatory first principle calculation.

In the present work, we use a sequential QM/MM method to study the solvent effects on the solvatochromic shifts of polar and non-polar molecules, acetone and benzene, dissolved in ambient water (AW) and supercritical water (SCW). Acetone is a simple molecule where the change of the n$\rightarrow \pi^*$ transition in water is well characterized by experiments[16,29–32] and has also been subjected to many theoretical studies.[33–42] Benzene is an important solute model because it is a key component of the amino acid phenylalanine and can serve as a simplified model for the aromatic structures of the bases of nucleic acids. Considering benzene's prototype of aromatic compounds, the study of benzene dissolved in SCW is also very useful for the application of SCW in toxic organic compound waste treatment. Therefore, the hydration structures and solvatochromic shift of benzene in AW and SCW have also attracted considerable research interests from the experimentalists[19,43] and theoreticians.[44–58] In the most past QM/MM calculations, only the solute molecule is treated quantum mechanically (see, e.g., Refs. 37 and 39) While the interactions between the polar acetone molecule and solvent water molecules are dominated by the classical electrostatic Coulomb repulsions, those between the non-polar benzene molecule and solvent water molecules are mainly ascribed to the quantum dispersion interactions. Therefore, we specially address the solute-solvent exchange-correlation effect in the QM/MM calculations by straightforwardly using larger sized QM region for the purpose of reasonably producing the electronic structure of solvated molecules, in particular for the non-polar solutes dissolved in water. In QM calculations based on the geometrical configurations selected from molecular dynamics (MD) trajectories, we use the time-dependent density functional theory (TDDFT) method[59,60] for a supra-molecule consisting of the solute molecule with its nearest neighbor water molecules while the other solvent molecules are considered as simple point charges. The dependencies of calculated electronic spectral shift on the QM supra-molecule size and the simple point charge background region's size as well as effect of the functional's long-range and dispersion corrections are carefully investigated. The outline of this paper is as follows. In Sec. II, we present a brief account of simulation and computational methodology adopted for the theoretical study of the excited states of acetone and benzene dissolved in water. Results for the hydration structure and the solvatochromic shifts of acetone and benzene under both ambient and supercritical conditions are analyzed in Sec. III. Concluding remarks are offered in Sec. IV.

II. COMPUTATIONAL METHODS

A. MD simulations

We use optimized potentials for liquid simulations (OPLS)[61] potential energy parameters for benzene and acetone and the rigid simple point charge extended (SPC/E) pair potential[62] for water molecules. The intermolecular interaction between a pair of molecules is

$$U_{pair} = \sum_i \sum_j 4\epsilon_{ij}\left[\left(\frac{\sigma_{ij}}{r_{ij}}\right)^{12} - \left(\frac{\sigma_{ij}}{r_{ij}}\right)^{6}\right] + \sum_i \sum_j \frac{q_i q_j}{4\pi\epsilon_0 r_{ij}}. \quad (1)$$

The first term is the Lennard-Jones potential energy of interaction evaluated between the atom sites on distinct molecules and the second term is the sum of electrostatic potential energies of interaction between the charges on sites i and j of distinct molecules. Here q_i is the charge on site i and r_{ij} is the distance between the sites i and j. Summaries of important non-bonded energy parameters for the solute and solvent are given in Table I. The coupling term σ_{ij} can be calculated as the arithmetic mean of the atom-type specific σ_{ii} parameters and ϵ_{ij} is calculated as the geometric mean of the ϵ_{ii} parameters. In the SPC/E model of water the OH bond distances are constrained at 1.0 Å and the bond angle between the two OH bonds is fixed at 109.47°.

The MD simulations are performed for aqueous solutions of benzene and acetone under ambient and supercritical conditions. Ambient condition is simulated with $T = 298$ K and $\rho = 0.99$ g/cm^3. The supercritical conditions are modeled with $T = 666$ K and 653 K for aqueous benzene and aqueous acetone, respectively, which for SCW ($T_c = 647.1$ K, $\rho_c = 0.322$ g/cm^3) correspond to a reduced temperature $T_r = T/T_c = 1.03$ or 1.009. A series of states with densities varying from 0.01 to 3.00 ρ_c are studied for the investigation of supercritical conditions. For each set of the density and temperature, one benzene molecule and 826 water molecules or one acetone molecule and 784 water molecules are located in a cubic cell replicated in three dimensions by the periodic boundary conditions and a NVT ensemble (isochoric-isothermal conditions) molecular dynamic simulation with a Nosé-Hoover thermostat[63,64] is carried out. The long-range Coulomb interactions are treated using the Ewald summation algorithm,[65]

TABLE I. Non-bonded energy parameters of SPC/E water model and OPLS acetone and benzene model.

	Water (SPC/E)		Benzene (OPLS)		Acetone (OPLS)			
n	O	H	C	H	C(R_2CO)	O(R_2CO)	C(RCH_3)	H(RH)
σ_{ii}(Å)	3.165	0.0	3.55	2.42	3.75	2.96	3.5	2.5
ϵ_{ii}(kcal mol^{-1})	0.1553	0.0	0.07	0.03	0.105	0.210	0.066	0.030
q_i(e)	− 0.8476	0.4238	− 0.115	0.115	0.47	− 0.47	− 0.18	0.06

and a cutoff distance of 1.2 nm is applied to the van der Waals (vdW) interactions for all cases. The MD equations of motion are integrated using the leapfrog-type Verlet algorithm with a 1 fs time step. Simulation configuration sets are collected every 500 steps for data analysis. In addition, the intramolecular geometry of the species is constrained during the simulations by using the SHAKE method.[66] The total simulation duration for an individual system is about 2 ns, in which the initial 1 ns simulation is used for the system equilibrium.

B. QM/MM calculation of electronic excited states in solution

In the sequential MD/QM treatment, we select 100 configurations separated by 10 ps for the QM/MM electronic structure calculations from the proceeding MD trajectories. In our QM/MM calculations, we use the electronic polarization embedding scheme,[67] by which the polarization of the QM subsystem by the charges residing on the MM atoms of the classically treated solvent molecules can be incorporated. This polarization is described by renormalizing the one-electron part of the effective Hamiltonian for the QM subsystem, allowing polarization of the QM wavefunction by the MM charges.

In our QM/MM calculations, we define a supra-molecule composed of the central solute molecule and its nearest N_{water}^{QM} water molecule neighbors instead of only one solute molecule as the QM part while the other solvent water molecules within a sphere with a cutoff radius r_{cutoff} are described as SPC/E simple point charges. The QM calculations of electronic excited states are performed using the TDDFT method as implemented in GAUSSIAN 09 program,[68] and the Becke-Lee-Yang-Parr (BLYP) functional[69–71] and the B3LYP hybrid functional[72–74] as well as the recently proposed long-range corrected hybrid functional ωB97X[75] and long-range corrected hybrid functional with dispersion corrections ωB97X-D[76] are employed with the 6-31+G(d) basis set.

III. RESULTS AND DISCUSSION

A. Solvatochromic shifts under ambient conditions

Before the study of the solvatochromic shift, we illustrate in Fig. 1 the radial distribution functions (RDFs) of the solute-solvent pairs for aqueous acetone and aqueous benzene under ambient conditions to study the microscopic solvation structure of the hydrated acetone and benzene. For the ambient aqueous acetone, $g_{O–O}$ ($g_{O–H}$) has the first peak at 2.75 (1.80) Å, indicating the hydrogen-bonding formed between the acetone oxygen and the water hydrogen. At the same time, the second peak is less structured. For the ambient aqueous benzene, the low-lying first peak of $g_{COM–O}$ ($g_{COM–H}$) may be ascribed to the π-hydrogen bonding[77–79] and the second main peak corresponds to a more general solvent shell. In computational studies, the average hydrogen-bonding number N_{HB} and the coordination number for the arrangement of water

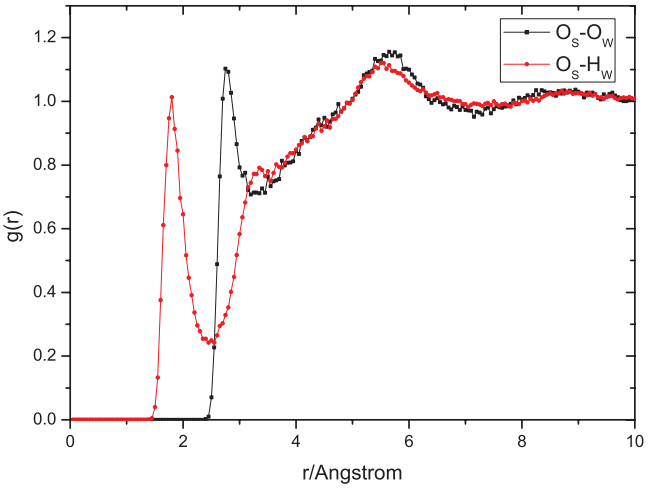

(a)

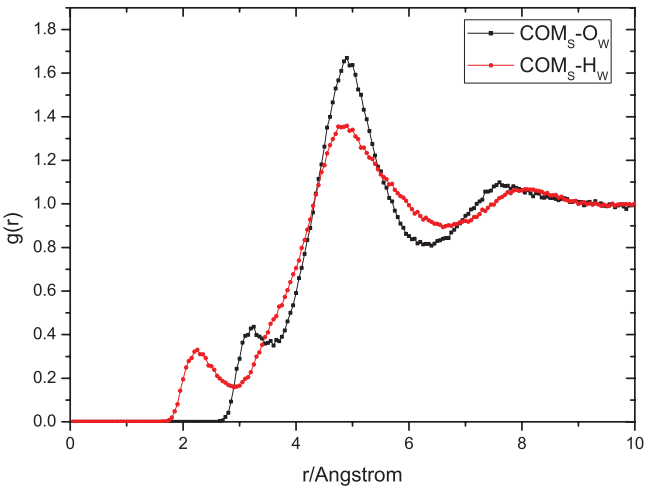

(b)

FIG. 1. Calculated radial distribution functions (RDFs) for O_S-O_W and O_S-H_W pairs in aqueous acetone (a) and COM_S-O_W and COM_S-H_W pairs in aqueous benzene (b) under ambient conditions (T = 298 K and ρ = 0.99 g/cm^3). (O_S and COM_S denote the solute's oxygen atom and the center of mass, while O_W, H_W represent the oxygen and hydrogen atoms of water solvents, respectively.)

molecules around the central solute molecule N_{Coor} can be calculated by the integration of $g_{\text{O–H}}$ ($g_{\text{COM–H}}$) or $g_{\text{O–O}}$ ($g_{\text{COM–O}}$) in the first peak as

$$N_{\text{HB}} = 8\pi\rho \int_0^{r_{\text{O–H}}^{\min}} g_{\text{O–H}}(r) r^2 \text{d}r, \tag{2}$$

$$N_{\text{Coor}} = 4\pi\rho \int_0^{r_{\text{O–O}}^{\min}} g_{\text{O–O}}(r) r^2 \text{d}r, \tag{3}$$

where ρ is the number density of the solution and $r_{\text{O–H}}^{\min}$ ($r_{\text{O–O}}^{\min}$) is the distance when the respective RDF minimum locates. From Fig. 1, the integrations up to the first minimums (around 2.45 Å for $g_{\text{O–H}}$ and 3.45 Å for $g_{\text{O–O}}$) of aqueous acetone give N_{HB} and N_{Coor} to be 1.6 and 2.8, respectively, similar to the previous simulation results.[37,39,80–82] Because the proportion of N_{HB} to N_{Coor} ($N_{\text{HB}}/N_{\text{Coor}}$) has been found to be nearly invariant during the variation of the bulk density,[82] we will only focus on the density dependence of N_{Coor} later. The integration up to the first minimum (3.6 Å) of $g_{\text{COM–O}}$ for aqueous benzene gives a coordination number of 1.2 oxygen atoms, and the integration up to the second minimum (6.4 Å) gives a coordination number of 33 oxygen atoms, very close to Mateus *et al.*'s recent OPLS-AA/TIP3P simulation.[56] Overall, our calculated collective coordination behavior for both hydrated acetone and benzene is in reasonable agreements with previous molecular simulations.

As a first step to study the solvatochromic shift, we perform the analysis of the influences of N_{water}^{QM} and r_{cutoff} values on the calculated electronic spectral shifts. Figure 2 shows the variations of aqueous acetone's and aqueous benzene's solvatochromic shifts $\Delta\nu$ under ambient conditions with different N_{water}^{QM} water molecule number in the QM region and different cutoff radius r_{cutoff} values for background simple point charge region. The quality of our present electronic structure calculations can be verified by the comparison with the experimental results. The experiments observed blueshifts with $\Delta\nu$ of 1500–1800 cm^{-1} (Refs. 29–32) for n→ π^* excitation of aqueous acetone and redshifts of about 143 cm^{-1} (Ref. 43) for π → π^* excitation of aqueous benzene. Our calculations with $N_{water}^{QM} = 36$ and $r_{cutoff} = 20$ Å give values of 1404 and -161 cm^{-1} for aqueous acetone and aqueous benzene, respectively, in very good accordance with experimental results. It is clearly shown in Fig. 2 that, the calculated values by $r_{cutoff} = 10$ Å differ remarkably with those by $r_{cutoff} = 15$ or 20 Å while $r_{cutoff} = 15$ and 20 Å can give very close results. This can be understood from the fact that the Coulomb electrostatic interactions between the solute and the solvent molecules are very long ranged. As a result, a sufficiently large point charge background with a radius no less than 15 Å is essential for a subsystem QM calculation to simulate bulk electronic properties. This is in agreement with the recent finding by Olbrich and Kleinekathöfer,[83] which states one actually needs to take all charges within a 20 Å radius around each chromophore into account for the results to converge. At the same time, from Fig. 2 one may also notice that the calculated solvatochromic shift value might be sensitive to the QM region size N_{water}^{QM}. For aqueous acetone, the calculation with the solute-only QM region ($N_{water}^{QM} = 0$)

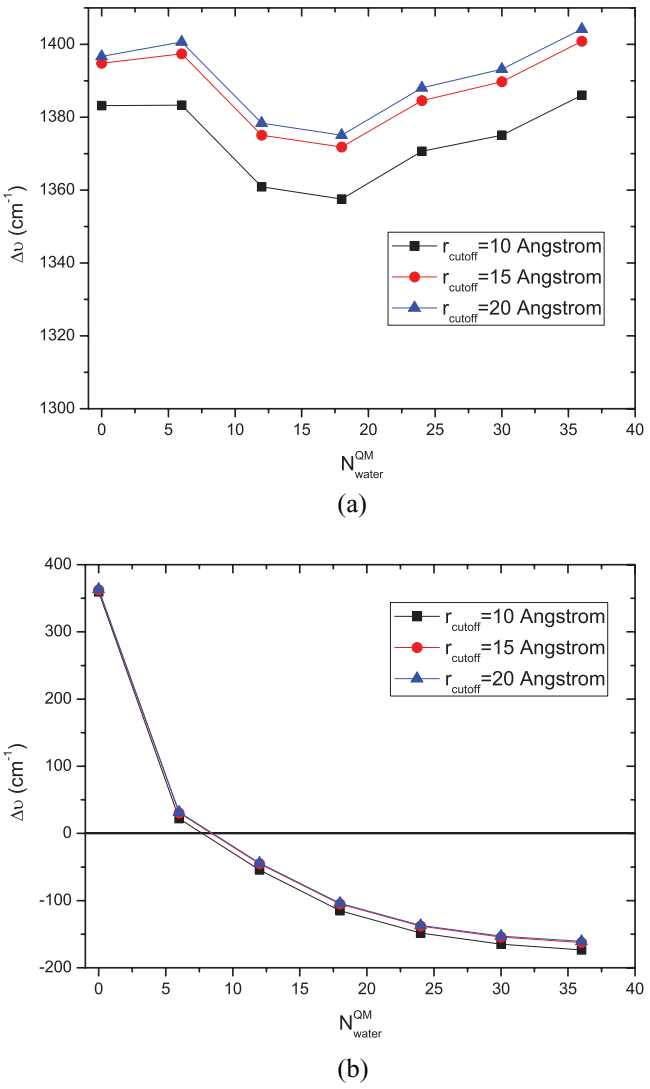

FIG. 2. Calculated solvatochromic shift $\Delta\nu$ of aqueous acetone (a) and aqueous benzene (b) under ambient conditions by TDDFT at ωB97X-D/6-31+G* level versus varying N_{water}^{QM} water molecule number in the QM region.

which accounts only the classical electrostatic interactions between the solute and solvent molecules give nearly the same $\Delta\nu$ value as that by calculations with a large QM region ($N_{water}^{QM} = 36$). Further inclusion of more nearest water molecules around the solute into the QM region does not lead to much change for the spectral shift. This verifies that the solute-solvent interactions for the polar solute dissolved in water are mainly dominated by the classical electrostatic interaction contributions. For aqueous benzene, the solvatochromic shift's dependence on the QM region size N_{water}^{QM} is more significant. $\Delta\nu$ is shown to change from blueshift to redshift with the increasing N_{water}^{QM} number and only gets nearly converged with $N_{water}^{QM} \simeq 30 \sim 36$. This demonstrates that a large QM region with $N_{water}^{QM} \geq 30$ is vital for describing the electronic excited state calculation of aqueous benzene. In fact, such a necessary $N_{water}^{QM} \geq 30$ value is approximately the coordination number, 33, of water in the first solvation shell around the central benzene molecule which has been shown in the earlier RDF and coordination number analysis. This shows that the exchange and correlation between the solute

TABLE II. Solvatochromic shift (cm^{-1}) of acetone and benzene in AW calculated with different QM region sizes and different density functionals. Background point charge region is set with a $r_{cutoff} = 20$ Å.

	Acetone				Benzene			
N_{water}^{QM}	BLYP	B3LYP	ωB97X	ωB97X-D	BLYP	B3LYP	ωB97X	ωB97X-D
0	1182	1345	1417	1397	390	388	352	364
6	307	1215	1430	1401	− 1005	− 89	− 6	32
12	− 127	1164	1405	1378	− 2678	− 234	− 113	− 44
18	− 608	1149	1397	1375	− 4230	− 423	− 205	− 104
24	− 1091	1159	1405	1388	− 5475	− 631	− 261	− 137
30	− 1471	1163	1407	1393	− 6557	− 801	− 290	− 153
36	− 2003	1174	1417	1404	− 7645	− 967	− 306	− 161

and solvents within the first solvent shell are non-neglectable although the aqueous benzene is a weakly coupled molecular aggregate system. A sufficient large QM region is extremely important for the correct simulation of non-polar molecules dissolved in polar solvents.

Obviously, calculated solvatochromic shifts should be dependent on the chosen simple point charge values used in the electronic embedding scheme of QM/MM. To check $\Delta\nu$'s dependence on the chosen simple point charge values used in the electronic embedding scheme of QM/MM, we also perform a series of QM/MM calculations with solute-only QM region ($N_{water}^{QM} = 0$) in which the nearest 36 water molecules use the Mulliken charges obtained from a preliminary QM/MM ($N_{water}^{QM} = 36$) calculation while the other outer solvent molecules still use SPC/E charges. Such kind of new QM/MM calculations with optimized nearest neighbor solvent charges give $\Delta\nu$ values of 1892 and 439 cm^{-1} for aqueous acetone and aqueous benzene, respectively. They are close to our standard QM/MM calculated values with solute-only QM region, 1397 and 364 cm^{-1} for aqueous acetone and aqueous benzene, respectively, implying that QM/MM calculations with different point charge values still present qualitatively similar descriptions for the solvatochromic shifts. Evidently, $\Delta\nu$'s difference between two sets of QM/MM calculations for hydrated acetone, 495 cm^{-1} is much larger than that for hydrated benzene, 75 cm^{-1}. Such larger $\Delta\nu$'s sensitivity to the chosen point charge values for hydrated acetone can be ascribed to the fact that the electrostatic interactions between polar solute and polar solvents should be much stronger than those between non-polar solute and polar solvents. Although there are still noticeable distinctions between the QM/MM results with different point charge values, such influence will be relatively small for our trend analysis of solvatochromic shifts because we use large QM regions ($N_{water}^{QM} = 36$) where the closest solvent molecules have been included in the QM part.

It is well known that the density functional theory (DFT) or TDDFT calculated results are much dependent on the chosen functional. In Table II we list the calculated electronic spectral shift values of ambient hydrated acetone and hydrated benzene by four different functionals: the pure BLYP functional, the B3LYP hybrid functional, and the long-range corrected ωB97X functional as well as long-range corrected ωB97X-D functional with dispersion correction. Obviously, the calculated results by the pure BLYP functional deviate drastically from the ωB97X-D results and the experimental determinations. The large errors of BLYP calculations should be attributed by the underestimation of non-local long-range electron-electron exchange interactions by the pure density functionals which may be impossible to be represented by a functional of a one-electron quantity. From Table II, the hybrid functional B3LYP with a inclusion of part exact non-local Hartree-Fock exchange is found to present qualitative correct shifts of $n \rightarrow \pi^*$ transitions of hydrated acetone and $\pi \rightarrow \pi^*$ of hydrated benzene, but it still underestimates the excitation energies. The large discrepancies between B3LYP results and experimental values for hydrated benzene are due to the fact that such popular traditional functionals are generally developed for modeling strong intermolecular interactions between solid macromolecular systems while the description of long-range dispersion interactions is not accurate. It is well known that the standard approximate exchange-correlation functionals underestimate the excitation energies for Rydberg states and charge-transfer states as well as extended π-conjugated systems and weakly interacting molecular aggregates, because they do not exhibit the correct $1/r$ asymptotic behavior but decay too rapidly. Such drawbacks may be overcome by the recent developments of long-range corrected exchange-correlation density functionals.[75,84–96] It can be seen from Table II that, the long-range corrected ωB97X functional gives more reasonable solvatochromic shifts than the pure BLYP and hybrid B3LYP functions although it still exaggerates the red spectral shift of aqueous benzene. Such overestimation of aqueous benzene's solvatochromic shift by wB97X may be due to its inappropriate treatment of quantum dispersion interactions. The van vdW intermolecular bondings are supposed to be in the balance of dispersion attraction and long-range exchange repulsion interactions, the latter of which has been well accounted and the former of which is still missing in the long-range corrected density functionals such as ωB97X. Recent efforts have offered possibilities to account for dispersion effects within DFT with the newly developed dispersion corrected exchange-correlation functionals.[76,97–101] ωB97X-D[76] is such a functional which includes both long-range corrections and dispersion corrections and recent benchmark calculations by Steinmann and Corminboeuf[102] have found it to be the best one among dozens of currently popular density functional for reproducing the intermolecular binding energies of two sets

of neutral and radical π-conjugated complexes in which the vdW interactions contribute substantially. Because dispersions arising from the instantaneous correlated movements of electrons are dependent on the polarizability of atoms or molecules, the dispersion effect is significant between atoms or molecules with more delocalized electron clouds, such as π-conjugated molecules such as benzene. Also considering that the electrostatic interactions between benzene and solvent molecules are much smaller than that between acetone and solvent molecules, the contribution of dispersion effect to the solvatochromic shift of aqueous benzene should be much more important than that of aqueous acetone. The differences between ωB97X results and ωB97X-D results for hydrated acetone and benzene illustrated in Table II clearly confirm the above analysis. This signifies the necessity of including both long-range corrections and dispersion corrections to the exchange-correlation density functionals for the accurate DFT calculations of weakly interacting molecular systems, especially the systems containing non-polar molecules.

For the popular QM/MM calculations with solute-only QM region ($N_{water}^{QM} = 0$), fixed charge model ignores the instantaneous solvent charge redistribution due to the solute electronic excitation. Such solvent polarization effect on the spectral shift can be included by virtue of using polarizable solvent models[103,104] which perform self-consistent solvent dipole calculations for both the ground state and the excited state. Recent studies by Lin and Gao[39] with such a polarizable model found the solvent polarization effect has a very small contribution (-37 cm^{-1}) to the total solvatochromic shift of aqueous acetone. Because our QM region includes not only the central solute but also its nearest N_{water}^{QM} solvent molecules, it is expected that the majority of the solvent polarization effect is included provided that a large N_{water}^{QM} value is used. From the ωB97X-D results listed in Table II, one may notice that the calculated $\Delta\nu$'s change is very small with the increasing QM region size for aqueous acetone, in consistence with Lin and Gao's conclusion[39] that the solvent charge redistribution following the solute excitation has a small contribution to the total spectral shift of aqueous acetone. On the contrary, $\Delta\nu$ changes much with the increasing QM region size for aqueous benzene, implying that solvent polarization effect impacts the solvatochromic shift of non-polar solutes dissolved in water more evidently. Such larger solvent polarization effect for hydrated benzene is induced by the much stronger quantum dispersion interactions between π-conjugated benzene and water solvent molecules which we have mentioned earlier. Therefore, QM/MM calculations with sufficiently large QM regions are necessary for the description of significant solvent polarization effect in the case of non-polar solute dissolved in polar solvents. Alternatively, such effect can also be included by QM/MM calculations with solute-only regions coupled with polarizable force fields and polarization embedding.[103,104]

B. Solvatochromic shifts under supercritical conditions

Now, let us turn our focus to the solvatochromic shift behavior of aqueous acetone and acetone benzene under supercritical conditions. Calculated $\Delta\nu$ for n $\rightarrow \pi^*$ of hydrated acetone and $\pi \rightarrow \pi^*$ of hydrated benzene by the electronic embedding scheme of QM/MM (ωB97X-D/6-31+G(d), $N_{water}^{QM} = 36$ and $r_{cutoff} = 20$ Å) are plotted as a function of reduced density ρ_r in Fig. 3. Interestingly, one may find three distinctive regions for both aqueous acetone and aqueous benzene. In the low-density gas-like region, the density increase is usually accompanied by a rapid rising blueshift (or redshift) in $\Delta\nu$. Then it is followed by a slowly rising plateau in the medium-density supercritical region. In the third stage, the increasing density induces steep shift increase. Such three stepwise behavior agrees well with the experimentally observed density dependence of $\Delta\nu$ by UV absorption spectroscopy.[16,19] Encouragingly, the quantitative magnitude of our calculated $\Delta\nu$ is also in reasonable accordance with the experimental determinations.[16,19] For example, our calculated $\Delta\nu$ values within the medium-density plateau region are around 600 and -125 cm^{-1} for aqueous acetone and aqueous benzene, respectively, close to the experimental determinations of about 600 and -80 cm^{-1}.[16,19] Earlier study by Lin and Gao[39] has ascribed

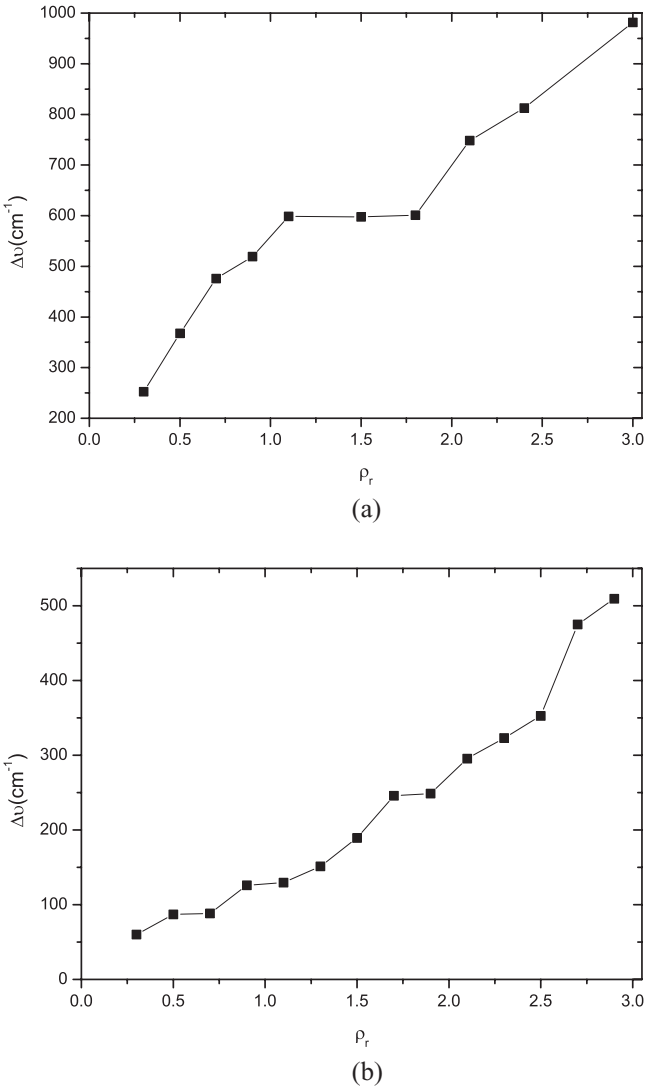

FIG. 3. Calculated solvatochromic shift $\Delta\nu$ versus the reduced density ρ_r for aqueous acetone (a) at $T = 666$ K and aqueous benzene (b) at $T = 653$ K.

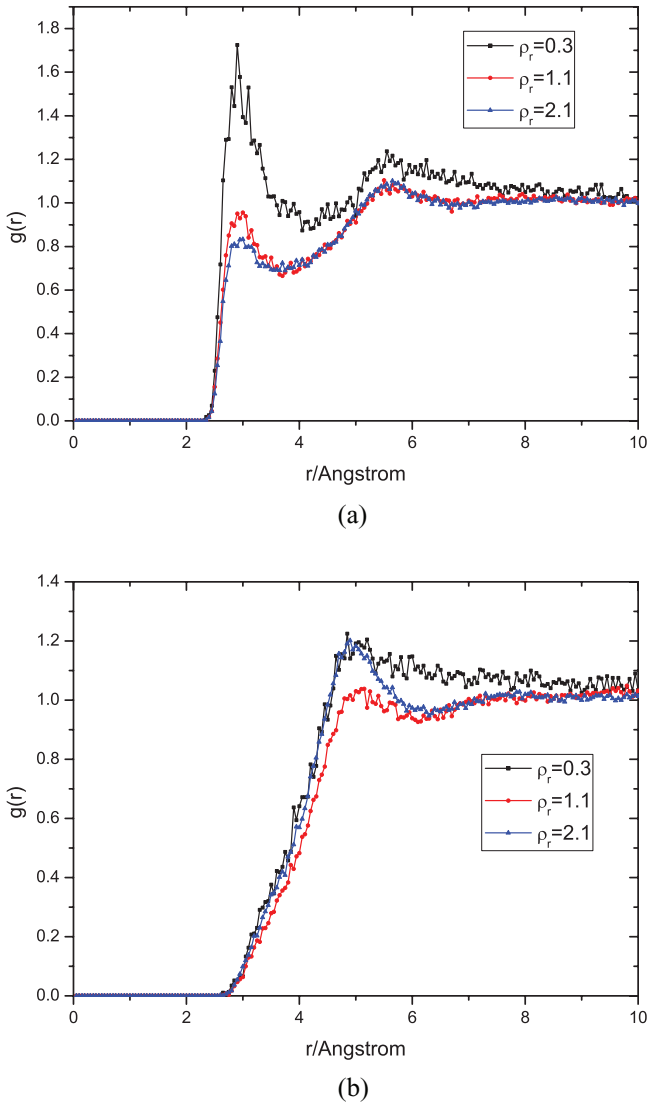

FIG. 4. Calculated RDFs for O(acetone)–O(water) pair in aqueous acetone and COM(benzene)–O(water) pair in aqueous benzene under high temperatures.

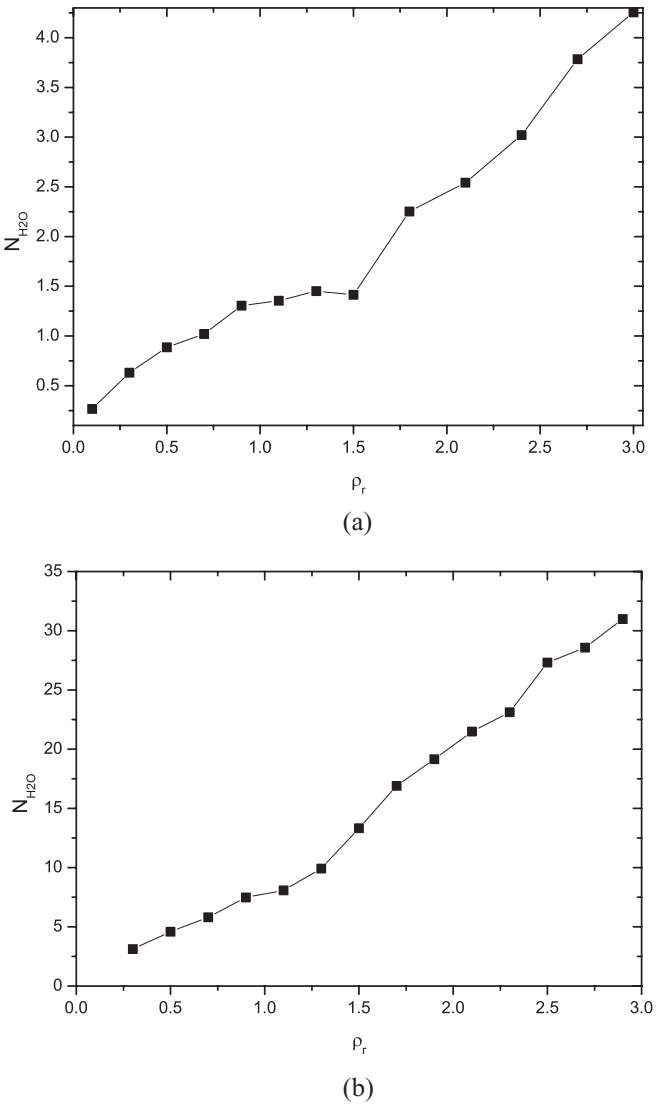

FIG. 5. Calculated coordination number in the first solvation shell N_{H_2O} versus the reduced density ρ_r for aqueous acetone (a) at $T = 666$ K and aqueous benzene (b) at $T = 653$ K.

the plateau of $\Delta\nu$ in the supercritical region to the solvent clustering around the solute, which is a fundamental microscopic phenomenon of SCFs and plays important roles in determining the physicochemical properties of organic solute in SCFs. The $\Delta\nu$ plateau of aqueous benzene is not so evident as that of aqueous acetone because interactions between the non-polar benzene and the polar water solvents are relatively weaker and accordingly the solvent clustering phenomenon around the solute is not remarkable. To find the microscopic clustering structure and its relationship with solvatochromic shifts, we will present structural analysis as follows.

In Fig. 4, we illustrate the RDFs of $g_{acetone-O}$ and $g_{benzene-O}$ for aqueous acetone and aqueous benzene under different high temperature conditions. We may clearly see the density dependence of the peak intensity for both cases. One may also notice the disappearance of a low-lying peak around r = 3.3 Å for hydrated benzene which corresponds to the weak π-HBs in ambient aqueous benzene in Fig. 1. This signifies the disappearance of π-HBs under high temperatures. To study the collective coordination behavior of the hydrated acetone and benzene, we integrate the water molecules up to the first minimum of RDF. We plot the calculated coordination number of water molecules in the first solvation shell as a function of reduced density ρ_r in Fig. 5. As expected, the changing trends of the coordination number of the first solvation shell reproduce those of the spectral shifts in Fig. 3. The plateau or the slowly changing around the critical density illustrated in Fig. 5 confirms the microscopic clustering of the solvents around the solute under supercritical region. As we have mentioned earlier, the first solvation shell of aqueous acetone is mainly caused by the hydrogen bonding formed between the acetone oxygen and the water hydrogen, which of course contributes the most important part of the solute-solvent interactions and accordingly the spectral shift. For the aqueous benzene, considering the π-hydrogen bonding diminishes under high temperatures and electrostatic interactions are very weak between non-polar solute and

water molecules, the vdW interactions between the solute and the solvent molecules in the first solvation shell should contribute the most important part of the solute-solvent interactions and accordingly the spectral shift. Therefore, the coordination number change of water molecules in the first solvation shell reproduces the solvatochromic shift change nicely for both aqueous acetone and aqueous benzene.

IV. SUMMARY AND CONCLUSION

We have investigated the hydration structures and the electronic spectral shifts of polar and non-polar solute molecules (acetone and benzene) dissolved in AW and SCW by isochoric-isothermal MD simulations with OPLS and SPC/E model potentials and subsequent QM/MM excitation energy calculations.

We report statistical mechanically averaged electronic excitation energies calculated with TDDFT method for 100 configurations generated from MD trajectories. From the detailed analysis of the dependence of the QM region size and point charge background region size as well as the different functionals, it is found that the inclusion of the solvent molecules within the first solvation shell into the QM region to account for the exchange-correlation between a solute and neighboring solvent molecules is important for the highly accurate spectral shift calculations, especially vital for the non-polar solutes whose interactions with the solvents are dominated by the quantum dispersions. At the same time, sufficiently large surrounding partial charge region ($r_{cutoff} \geq 15$ Å) as well as the functional corrections to describe the long-range dispersion-corrections are also essential for the study of the electronic excited states in condensed phase. With reasonable chosen computational scheme (ωB97XD/6-31+G(d) calculation with $r_{cutoff} = 20$ Å and $N_{water}^{QM} = 36$), our calculated solvatochromic blueshift of ambient aqueous acetone is 1404 cm^{-1}, in close agreement with the experimentally determined values, 1500–1800 cm^{-1}. For the non-polar solute of benzene in AW, we find the dispersion-induced redshift of 161 cm^{-1}, in reasonable accordance with the experimentally determined value, 143 cm^{-1}. This indicates that sound theoretical studies of solvatochromic shift can be achieved provided that a reasonable computational scheme with sufficiently large N_{water}^{QM} and r_{cutoff} values is implemented.

We also examine the density dependence of solvatochromic shifts of aqueous acetone and aqueous benzene at high temperatures. Both of them are found to present three distinctive regions: low-density gas-like region, supercritical region, and high-density liquid-like region, although this is not so evident in the case of aqueous benzene due to the weak solute-solvent interactions. Both the qualitative trend and the quantitative magnitude of our calculated shifts are in excellent agreements with the experimental observations. The plateau behavior of solvatochromic shift in the supercritical region is ascribed to the solvent clustering around the solute, which is a fundamental phenomenon of SCFs. The density dependence of our calculated coordination number of the first solvation shell nicely reproduces the trend of spectral shift and verifies the solvent clustering phenomenon of SCFs and its relationship with SCF's physicochemical properties.

ACKNOWLEDGMENTS

This work is supported by the National Natural Science Foundation of China (Grant Nos. 21003072 and 91122019), National Basic Research Program (Grant No. 2011CB808604), and the Fundamental Research Funds for the Central Universities.

[1] L. T. Taylor, J. Supercrit. Fluids **47**, 566 (2009).
[2] M. Goto, J. Supercrit. Fluids **47**, 500 (2009).
[3] F. Cansell and C. Aymonier, J. Supercrit. Fluids **47**, 508 (2009).
[4] A. H. Romang and J. J. Watkins, Chem. Rev. **110**, 459 (2010).
[5] H. Weingärtner and E. U. Franck, Angew. Chem., Int. Ed. **44**, 2672 (2005).
[6] P. Munshi and S. Bhaduri, Curr. Sci. **97**, 63 (2009).
[7] R. Ishii, S. Okazaki, I. Okada, M. Furusaka, N. Watanabe, M. Misawa, and T. Fukunaga, J. Chem. Phys. **105**, 7011 (1996).
[8] J. Benzler, S. Linkersdorfer, and K. Luther, J. Chem. Phys. **106**, 4992 (1997).
[9] D. J. Myers, R. S. Urdahl, B. J. Cherayil, and M. D. Fayer, J. Chem. Phys. **107**, 9741 (1997).
[10] T. I. Mizan, P. E. Savage, and R. M. Ziff, J. Phys. Chem. **100**, 403 (1996).
[11] S. Beuermann, M. Buback, C. Isemer, I. Lacik, and A. Wahl, Macromolecules **35**, 3866 (2002).
[12] D. Dellis, M. Chalaris, and J. Samios, J. Phys. Chem. B **109**, 18575 (2005).
[13] H. Ma and J. Ma, J. Chem. Phys. **135**, 054504 (2011).
[14] H. Ma, J. Chem. Phys. **136**, 214501 (2012).
[15] C. Reichardt, *Solvent Effects in Organic Chemistry* (Verlag Chemie, Weinheim/New York, 1979).
[16] G. E. Bennett and K. P. Johnston, J. Phys. Chem. **98**, 441 (1994).
[17] H. Oka and O. Kajimoto, Phys. Chem. Chem. Phys. **5**, 2535 (2003).
[18] M. Osada, K. Toyoshima, T. Mizutani, K. Minami, M. Watanabe, T. Adschiri, and K. Arai, J. Chem. Phys. **118**, 4573 (2003).
[19] N. Kometani, K. Takemiya, Y. Yonezawa, F. Amita, and O. Kajimoto, Chem. Phys. Lett. **394**, 85 (2004).
[20] H. Lin and D. G. Truhlar, Theor. Chem. Acc. **117**, 185 (2007).
[21] O. Tapia and O. Goscinski, Mol. Phys. **29**, 1653 (1975).
[22] S. Miertus, E. Scrocco, and J. Tomasi, Chem. Phys. **55**, 117 (1981).
[23] D. M. Chipman, J. Chem. Phys. **110**, 8012 (1999).
[24] A. Klamt and G. Schüürmann, J. Chem. Soc., Perkin Trans. 2 **2**, 799 (1993).
[25] A. Warshel and M. Levitt, J. Mol. Biol. **103**, 227 (1976).
[26] M. S. Gordon, M. A. Freitag, P. Bandyopadhyay, J. H. Jensen, V. Kairys, and W. J. Stevens, J. Phys. Chem. A **105**, 293 (2001).
[27] M. S. Gordon, L. V. Slipchenko, H. Li, and J. H. Jensen, Annu. Rep. Comp. Chem. **3**, 177 (2007).
[28] A. DeFusco, N. Minezawa, L. V. Slipchenko, F. Zahariev, and M. S. Gordon, J. Phys. Chem. Lett. **2**, 2184 (2011).
[29] N. S. Bayliss and E. G. McRae, J. Phys. Chem. **58**, 1006 (1954).
[30] N. S. Bayliss and G. Wills-Johnson, Spectrochim. Acta, Part A **24**, 551 (1968).
[31] W. P. Hayes and C. J. Timmons, Spectrochim. Acta **21**, 529 (1965).
[32] I. Renge, J. Phys. Chem. A **113**, 10678 (2009).
[33] J. Gao, J. Am. Chem. Soc. **116**, 9324 (1994).
[34] M. Cossi and V. Barone, J. Chem. Phys. **112**, 2427 (2000).
[35] F. Aquilante, M. Cossi, O. Crescenzi, G. Scalmani, and V. Barone, Mol. Phys. **101**, 1945 (2003).
[36] K. Coutinho and S. Canuto, J. Mol. Struct.: THEOCHEM **632**, 235 (2003).
[37] K. Aidas, J. Kongsted, A. Osted, K. V. Mikkelsen, and O. Christiansen, J. Phys. Chem. A **109**, 8001 (2005).
[38] T. L. Fonseca, K. Coutinho, and S. Canuto, J. Chem. Phys. **126**, 9034508 (2007).
[39] Y.-L. Lin and J. Gao, J. Chem. Theory Comput. **3**, 1484 (2007).
[40] A. V. Marenich, C. J. Cramer, and D. G. Truhlar, J. Chem. Theory Comput. **6**, 2829 (2010).
[41] Y.-K. Li, Q. Zhu, X.-Y. Li, K.-X. Fu, X.-J. Wang, and X.-M. Cheng, J. Phys. Chem. A **115**, 232 (2011).
[42] D. M. Chipman, J. Chem. Phys. **131**, 014104 (2009).
[43] N. S. Bayliss and L. Hulme, Aust. J. Chem. **6**, 257 (1953).
[44] J. Gao, J. Am. Chem. Soc. **115**, 6893 (1993).
[45] J. Zhou, W. Wang, and C. Zhong, Chin. J. Chem. Eng. **9**, 196 (2001).
[46] T. M. Raschke and M. Levitt, J. Phys. Chem. B **108**, 13492 (2004).
[47] C. Nieto-Draghi, J. B. Avalos, O. Contreras, P. Ungerer, and J. Ridard, J. Chem. Phys. **121**, 10566 (2004).

[48]P. Linse, J. Am. Chem. Soc. **112**, 1744 (1990).
[49]W. L. Jorgensen, E. R. Laird, T. B. Nguyen, and J. Tiradorives, J. Comput. Chem. **14**, 206 (1993).
[50]A. Laaksonen, P. Stilbs, and R. E. Wasylishen, J. Chem. Phys. **108**, 455 (1998).
[51]S. Urahata and S. Canuto, Chem. Phys. Lett. **313**, 235 (1999).
[52]P. Schravendijk and N. F. A. van der Vegt, J. Chem. Theory Comput. **1**, 643 (2005).
[53]P. E. M. Lopes, G. Lamoureux, B. Roux, and D. A. MacKerrell, J. Phys. Chem. B **111**, 2873 (2007).
[54]M. Allesch, E. Schwegler, and G. Galli, J. Phys. Chem. B **111**, 1081 (2007).
[55]M. Allesch, F. C. Lightstone, E. Schwegler, and G. Galli, J. Chem. Phys. **128**, 014501 (2008).
[56]M. P. S. Mateus, N. Galamba, and B. J. Costa Cabral, J. Chem. Phys. **136**, 014507 (2012).
[57]S. Urahata, K. Coutinho, and S. Canuto, Chem. Phys. Lett. **274**, 269 (1997).
[58]K. Coutinho, S. Canuto, and M. C. Zerner, J. Chem. Phys. **112**, 9874 (2000).
[59]E. Runge and E. K. U. Gross, Phys. Rev. Lett. **52**, 997 (1984).
[60]*Time-Dependent Density-Functional Theory – Concepts and Applications*, edited by C. A. Ullrich (Oxford University Press, New York, 2012).
[61]W. L. Jorgensen, D. S. Maxwell, and J. TiradoRives, J. Am. Chem. Soc. **118**, 11225 (1996).
[62]H. J. C. Berendsen, J. R. Grigera, and T. P. Straatsma, J. Phys. Chem. **91**, 6269 (1987).
[63]S. Nosé, J. Chem. Phys. **81**, 511 (1984).
[64]W. G. Hoover, Phys. Rev. A **31**, 1695 (1985).
[65]P. P. Ewald, Ann. Phys. **64**, 253 (1921).
[66]J. P. Ryckaert, G. Ciccotti, and H. J. C. Berendsen, J. Comput. Phys. **23**, 327 (1977).
[67]D. Bakowies and W. Thiel, J. Phys. Chem. **100**, 10580 (1996).
[68]M. J. Frisch, G. W. Trucks, H. B. Schlegel *et al.*, GAUSSIAN 09, Revision B.01, Gaussian, Inc., Wallingford, CT, 2009.
[69]A. D. Becke, Phys. Rev. A **38**, 3098 (1988).
[70]C. Lee, W. Yang, and R. G. Parr, Phys. Rev. B **37**, 785 (1988).
[71]B. Miehlich, A. Savin, H. Stoll, and H. Preuss, Chem. Phys. Lett. **157**, 200 (1989).
[72]A. D. Becke, J. Chem. Phys. **98**, 5648 (1993).
[73]P. J. Stephens, F. J. Devlin, C. F. Chablowski, and M. J. Frisch, J. Phys. Chem. **98**, 11623 (1994).
[74]R. H. Hertwig and W. Koch, Chem. Phys. Lett. **268**, 345 (1997).
[75]J.-D. Chai and M. Head-Gordon, J. Chem. Phys. **128**, 084106 (2008).
[76]J.-D. Chai and M. Head-Gordon, Phys. Chem. Chem. Phys. **10**, 6615 (2008).
[77]T. S. Zwier, Annu. Rev. Phys. Chem. **47**, 205 (1996).
[78]S. Suzuki, P. G. Green, R. E. Bumgarner, S. Dasgupta, W. A. Goddard, and G. A. Blake, Science **257**, 942 (1992).
[79]K. P. Gierszal, J. G. Davis, M. D. Hands, D. S. Wilcox, L. Slipchenko, and D. Ben-Amotz, J. Phys. Chem. Lett. **2**, 2930 (2011).
[80]M. E. Martin, M. L. Sanchez, F. J. Olivares del Valle, and M. A. Aguilar, J. Chem. Phys. **113**, 6308 (2000).
[81]M. A. Thompson, J. Phys. Chem. **100**, 14492 (1996).
[82]Y. Takebayashi, S. Yoda, S. Sugeta, K. Otake, T. Sako, and M. Nakahara, J. Chem. Phys. **120**, 6100 (2004).
[83]C. Olbrich and U. Kleinekathöfer, J. Phys. Chem. B **114**, 12427 (2010).
[84]T. Leininger, H. Stoll, H.-J. Werner, and A. Savin, Chem. Phys. Lett. **275**, 151 (1997).
[85]H. Iikura, T. Tsuneda, T. Yanai, and K. Hirao, J. Chem. Phys. **115**, 3540 (2001).
[86]Y. Tawada, T. Tsuneda, S. Yanagisawa, Y. Yanai, and K. Hirao, J. Chem. Phys. **120**, 8425 (2004).
[87]I. C. Gerber and J. G. Ángyán, Chem. Phys. Lett. **415**, 100 (2005).
[88]J. Toulouse, F. Colonna, and A. Savin, J. Chem. Phys. **122**, 014110 (2005).
[89]J. G. Ángyán, I. C. Gerber, A. Savin, and J. Toulouse, Phys. Rev. A **72**, 012510 (2005).
[90]E. Goll, H.-J. Werner, and H. Stoll, Phys. Chem. Chem. Phys. **7**, 3917 (2005).
[91]E. Goll, H.-J. Werner, H. Stoll, T. Leininger, P. Gori-Giorgi, and A. Savin, Chem. Phys. **329**, 276 (2006).
[92]O. A. Vydrov, J. Heyd, A. V. Krukau, and G. E. Scuseria, J. Chem. Phys. **125**, 074106 (2006).
[93]O. A. Vydrov and G. E. Scuseria, J. Chem. Phys. **125**, 234109 (2006).
[94]I. C. Gerber, J. G. Ángyán, M. Marsman, and G. Kresse, J. Chem. Phys. **127**, 054101 (2007).
[95]J.-W. Song, T. Hirosawa, T. Tsuneda, and K. Hirao, J. Chem. Phys. **126**, 154105 (2007).
[96]A. J. Cohen, P. Mori-Sánchez, and W. Yang, J. Chem. Phys. **126**, 191109 (2007).
[97]J. F. Dobson and B. P. Dinte, Phys. Rev. Lett. **76**, 1780 (1996).
[98]Y. Andersson, D. C. Langreth, and B. I. Lundqvist, Phys. Rev. Lett. **76**, 102 (1996).
[99]M. Kamiya, T. Tsuneda, and K. Hirao, J. Chem. Phys. **117**, 6010 (2002).
[100]T. Sato, T. Tsuneda, and K. Hirao, J. Chem. Phys. **123**, 104307 (2005).
[101]T. Sato, T. Tsuneda, and K. Hirao, J. Chem. Phys. **126**, 234114 (2007).
[102]S. N. Steinmann and C. Corminboeuf, J. Chem. Theory Comput. **8**, 4305 (2012).
[103]M. A. Thompson and G. K. Schenter, J. Phys. Chem. **99**, 6374 (1995).
[104]J. Gao and K. Byun, Theor. Chem. Acc. **96**, 151 (1997).